# Emergent Time Windows in Nonlinear Neural Models

Colleen Mitchell
Department of Mathematics
University of Iowa
14 MacLean Hall
Iowa City, IA 52242-1419

Michael Reed
Department of Mathematics
Duke University
Science Drive
Durham, NC 27708

## Abstract.

In order to study how $n$ to 1 convergence sharpens timing information, we have used a simple time-window (TW) model in which the target neuron fires the first time it has received $m$ action potentials in the previous $\varepsilon$ milleseconds. Although the TW is convenient for proving theorems and Monte-Carlo simulations, it is a natural question whether it represents well the physiological reality. We first present simulations that show, in the case $n = 3, m = 3$, that the Hodgkin-Huxley model has a very sharp time window but the leaky integrate-and-fire model (LIF) does not. Simulations also show that other non-linear models including quadratic-integrate-and-fire (QIF), the theta model, and the Fitzhugh-Nagumo model also have sharp time window behavior. We then give a complete analytical treatment of the LIF and QIF models to explain why the first does not have a sharp time window but the second does. This suggests that TW neurons may give a better approximation to physiological reality than LIF neurons.



**Keywords:** neural networks, time windows, timing precision, convergence,

**AMS subject classification:** 92, 60.

**Running head:** time windows

# 1. Introduction.

A fundamental issue in neurobiology is to understand how the central nervous system (CNS) can perform accurate and reliable calculations with neurons that are intrinsically variable and unreliable devices. A particular instance of this general problem is to understand how network and/or cellular properties can sharpen the timing of noisy inputs. This question has a long history in the auditory system ([37] [24] [29]) where auditory nerve (AN) fibers of mammals typically show standard deviations of latency (time to firing) of about 1 msec under repeated trials with the same sound. Yet, psychophysical experiments ([49][48][36]) have shown that mammals can detect extremely small binaural timing differences down to the low microsecond and even nanosecond range. This has been confirmed by physiological experiments ([19][40][41][12][20][16][35]) that show that certain classes of neurons in the brainstem have very small standard deviations of latency under repeated trials, even though these neurons are receiving information only from the same auditory nerve fibers that are such sloppy timers.

All fibers of the AN synapse on cells of the cochlear nucleus (CN) and some of these cells show "onset" responses, that is, they have low spontaneous rates and they fire a single spike in response to sounds after a time lag (called the latency). Often the latency in these cells (for example, octopus cells) has a much smaller standard deviation under repeated trials than the standard deviations of latency in the AN. Typically these cells receive many synapses from AN fibers (convergence) and it has long been thought that they sharpen timing by acting as coincidence detectors for these converging fibers. Young, Rothman and co-workers [50][43][44][45][46][47] conducted experiments and used numerical simulations of biophysical models to investigate how the response properties of CN neurons depend on the details of their channel kinetics and the convergence of inputs. Cai et al [10][11] used simulations of biophysical models to investigate the onset response of octopus cells. Burkitt and Clark [8][9] used numerical simulations of leaky integrate-and-fire models to study how convergence of inputs effects the onset response. Kalluri and Delgutte [25][26] have created a computational model using leaky integrate-and-fire models for the CN target cells and adaptively filtered Poisson processes to model spike trains along each of the convergent AN fibers. They are interested in determining what properties of the target cell, the filtered Poisson process in AN fibers, the convergence from AN fibers to the target, and adaptation in the hair cells cause the target neuron to have an onset response with low spontaneous rate. Gerstner et al [18] have studied similar issues in the avian nucleus laminaris. These numerical computations suggest strongly that there is a connection between the amount of convergence and the sharpening of timing information. However, the models are so elaborate and have so many parameters that it is difficult to make precise the mechanisms by which convergence sharpens timing.

For this reason, we have been studying a simpler model in which convergence and the sharpening of timing are isolated as the objects of study. There are $n$ identical input neurons and all receive the same stimulus. Each fires a single action potential at a time selected independently from a probability density $f$ with standard deviation 1 msec. The axons of the $n$ neurons are of equal length and project to one target neuron that fires a single action potential the first time that it has received $m$ inputs in the previous $\varepsilon$ msec. Of course, the target neuron may not fire at all in response to a particular stimulus. We denote the conditional density of the time of firing of the target neuron, given that it fires, by $g_{n,m,\varepsilon,f}$ and its standard deviation by $\sigma_{n,m,\varepsilon,f}$, since both will depend on $n$, $m$, $\varepsilon$, and $f$. If $\sigma_{n,m,\varepsilon,f} < 1$ msec, then we say that timing has been sharpened. A change of variables shows that there is a scaling law $\sigma_{n,m,\varepsilon,f} = s\sigma_{n,m,\frac{\varepsilon}{s},f_s}$, where $f_s(t) \equiv sf(st)$, so there is no loss in generality in taking the standard deviation of the input density $f$ to be 1 msec [38][32]. For obvious reasons we call a neuron with this firing rule a sharp time-window (TW) neuron

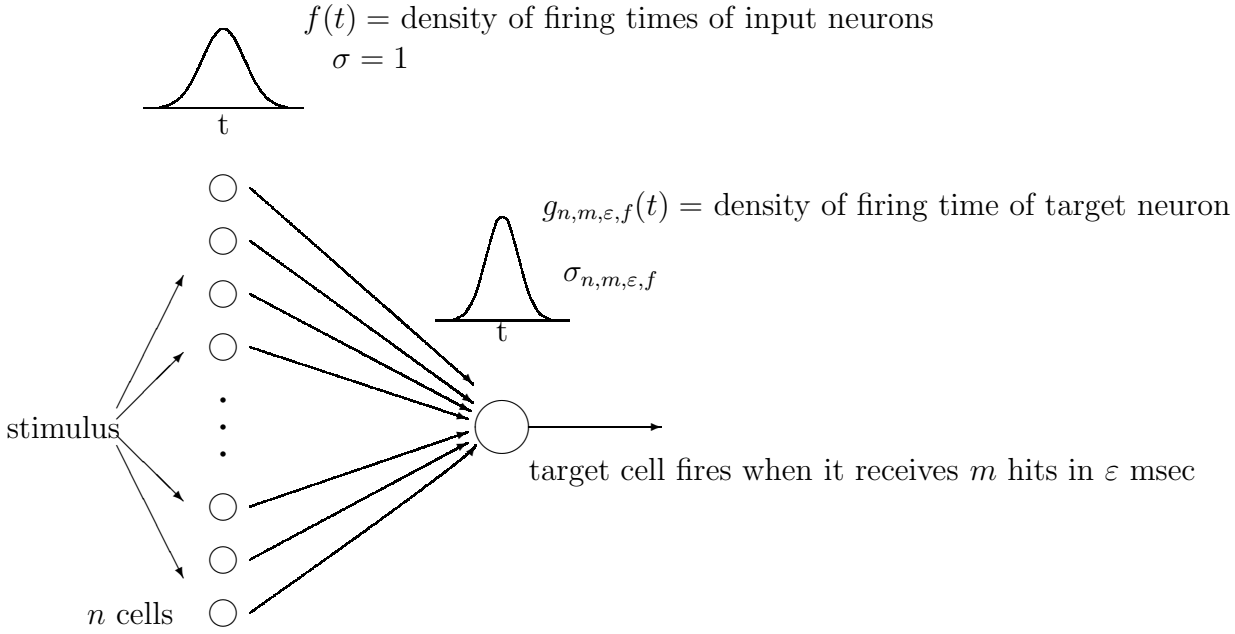


**Figure 1. The time window model.** $n$ cells receive the same input and fire at times that are selected independently from the density $f$, which has standard deviation $\sigma = 1$. All $n$ cells project to one target cell with equal length axons. The target cell fires (if and) when it has received $m$ action potentials in the previous $\varepsilon$ milleseconds. $g_{n,m,\varepsilon,f}$ is the density for the time of firing of the target cell (conditioned on success of firing). If its standard deviation, $\sigma_{n,m,\varepsilon,f}$, is less than one, then the convergence has sharpened timing.

The simplicity of the model has allowed us to use the tools of probability theory

and mathematical statistics to give examples and to prove theorems that make precise statements about the relationship between convergence and the sharpening of timing ([38][32][33][34]). It is widely believed in the auditory community that: (1) Raising $n$ sharpens timing; (2) Raising $m$ sharpens timing; (3) Decreasing $\varepsilon$ sharpens timing. We have given examples that show that none of these statements is true in general and we have characterized the sharpening of timing under particular hypotheses and in various asymptotic limits. In [34] we were able to use our theorems to explain how octopus cells in the cochlear nucleus sharpen timing.

Throughout this previous work we ignored the question of how well this simple model mimics the behavior of real neurons and real convergence networks, the issue that we turn to here. Do real neurons have sharp time windows? How well can the simple two parameter fire rule, "the target neuron fires the first time it receives $m$ inputs in the previous $\varepsilon$ msec," represent the full biophysical complexity of the target neuron? For reasons that we discuss below, we have been investigating these questions in the case $n = 3$, $m = 3$, that is, there are three converging fibers and two simultaneous hits are not enough to fire the target neuron but three nearly simultaneous hits will cause an action potential. Let $\ell$ denote the time between the first arriving hit and the third. Then, in our sharp time-window model the target neuron fires with probability 1 if $\ell \leq \varepsilon$ and fires with probability 0 if $\ell > \varepsilon$; note that it doesn't matter when the second hit arrives, just the time between the first and the third. If we let $P_{TW}(\ell)$ denote the probability of firing as a function of $\ell$, then $P_{TW}(\ell)$ is a step function that drops instantaneously from 1 to 0 at $\varepsilon = \ell$. In Section 2 we describe the corresponding function, $P_{HH}(\ell)$, for a Hodgkin-Huxley (HH) squid giant axon neuron with three afferent fibers computed using numerical simulations. Much to our surprise, $P_{HH}(\ell)$ looks very similar to $P_{TW}(\ell)$, so the HH neuron has a sharp time window, at least in the case $n = 3$, $m = 3$. We have done similar computations using other standard non-linear models for the target neuron. In each case, the model neuron has a sharp time window. We also performed the same simulations with leaky integrate-and-fire (LIF) neurons and they do not have sharp time windows. This suggests that, for a neuron that is the target of converging fibers, an TW neuron may give a better approximation to real neuronal behavior than an LIF neuron.

In order to understand this situation, we compute in Section 3 an explicit formula for $P_{LIF}(\ell)$, the probability of firing of an LIF neuron as a function of $\ell$ in the case $n = 3$, $m = 3$. Using the formula, it is easy to see why the LIF neuron does not have a sharp time window. Then, in Section 4, we compute the analogous function, $P_{QIF}(\ell)$, for a quadratic-integrate-and-fire (QIF) neuron. The QIF neuron does have a sharp time window and the explicit formula for $P_{QIF}(\ell)$ shows why. The QIF neuron has a stable equilibrium point at the origin and an unstable equilibrium point at a positive voltage. We believe that it is this property, shared by the HH neuron and most other non-linear models of excitable cells that causes these models to behave as though they have (approximately) sharp time windows.

These numerical and analytical calculations suggest that (at least some) real neu-

rons may have sharp time windows, an assertion that should be tested experimentally.

## 2. Computational Results.

In order to evaluate the degree to which various neural models exhibit time windows, we first present some computational results. We wish to compare the patterns of input times which will cause each type of model cell to fire. It is clear that if there are only two inputs, any model will respond as a time window neuron. That is, either the two inputs are sufficiently close together in time and the target cell fires or they are not and it doesn't. We therefore focus on the case with three inputs, the simplest case in which the models may differ. The strength of each input is identical and is chosen so that two inputs will not make the cell fire but all three will be sufficient if they are close enough together in time. Thus each input contributes $s$ mv and $s$ is between $\frac{1}{3}$ and $\frac{1}{2}$ of the threshold stimulus. In the terminology of the time window model, we call this case n=3, m=3. If the model neuron is a perfect time window neuron, it will fire with probability 1 if all three inputs are within $\varepsilon$ of each other and with probability zero if they are not. That is, if the time between the first input and the third input, which we call $\ell$, is at most $\varepsilon$, then the cell fires, and if $\ell > \varepsilon$ the cell does not fire. The probability of firing $P_{TW}$ as a function of $\ell$ is shown in Figure 2.

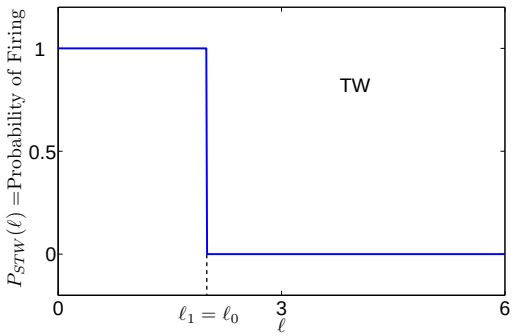


**Figure 2. Probability of firing as a function of $\ell$ for a Time Window target neuron.** The first action potential arrives at the target neuron at $t = 0$ and the third action potential arrives at $t = \ell$. The size of the time window is $\varepsilon = \ell_1 = \ell_0$, so if $\ell \leq \ell_1$ the target neuron fires with probability one, and if $\ell > \ell_0$ the target neuron does not fire. $\ell_1$ was chosen to match the computed $\ell_1$ for the Hodgkin-Huxley neuron (Figure 3).

Next we conduct the same experiment numerically with the Hodgkin-Huxley equations. We use the HH model with the original giant squid axon parameters [23]. We first determined the threshold stimulus that will elicit an action potential, then use three brief input stimuli, each 40% of this threshold. In this way, we guarantee that all three stimuli are required to trigger an action potential. For each value of $\ell$ we run the simulation with many different values for the time of the second input, which we call $x$. We assume that the second input is uniformly distributed between the

first and third inputs and again plot (Figure 3) the probability of firing $P_{HH}$ as a function of $\ell$. It is clear that the behavior of the HH neuron is similar to that of the Time Window neuron, if $\ell$ is less than some threshold value $\ell_1$, the HH model cell will fire, with probability one. If $\ell$ is between $\ell_0$ and $\ell_1$ the target cell will fire with some probability which does depend on $x$ and thus on the distribution of $x$. If $\ell$ is above $\ell_0$ the target cell will never fire, regardless of the value of $x$. Suprisingly, as in our time window model, the timing of the second hit $x$ makes very little difference and only effects the shape of the curve in the very narrow region of $\ell_1 < \ell < \ell_0$. To make the figures easy to compare we chose a value for $\varepsilon$ in Figure 2 that is close to the the observed threshold for $\ell$ in the HH model.

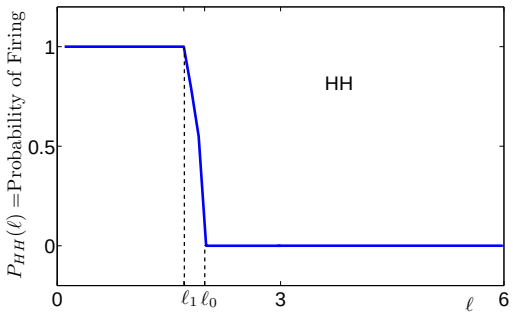


**Figure 3. Probability of firing as a function of $\ell$ for a Hodgkin-Huxley target neuron.** The first action potential arrives at the target neuron at $t = 0$ and the third action potential arrives at $t = \ell$. If $\ell \leq \ell_1$ the target neuron fires with probability one, and if $\ell > \ell_0$ the target neuron does not fire. $\ell_1$ and $\ell_0$ are quite close, so the Hodgkin-Huxley neuron behaves similarly to the time window neuron. The stimuli are short square pulses and each stimulus has an amplitude which is 40% of the amplitude required to elicit an action potential from a single stimulus.

Our computational tests found similar results in a large class of neural models including some simplified models such as the Theta model [15] and the FitzHugh-Nagumo model [17] as well as some more biophysically detailed models such as the Rothman-Manis model ([43][44][45]), a model of bushy cells in the cochlear nucleus. In all cases the interval $\ell_1 < \ell < \ell_0$ was very narrow indicating that the time of the intermediate hit had very little to do with the probability of firing and that all of these models have inherent time–window–like behavior. These models have in common that the target neuron fires when the voltage passes an unstable fixed point or unstable manifold.

We also conducted the same experiment using a Leaky-Integrate-and-Fire (LIF) model for the target neuron. Thus, an incoming action potential immediately increases the voltage, which then decays exponentially, and the model cell fires if a threshold is reached. Again, we chose a stimulus that is 40% of the threshold and for each value of $\ell$ varied the time of the second input uniformly between the time

of the first and third inputs. The behavior of the LIF is qualitatively very different; see Figure 4. There is not a steep drop from probability one to probability zero but rather a large range $\ell_1 < \ell < \ell_0$ in which there is a gradual decrease in the probability of firing. Note that this model has one additional parameter, the time constant $\tau$. This parameter can be thought of as scaling time and so different values of this parameter will simply rescale the $\ell$ axis in Figure 4. We therefore chose the value of $\tau$ so that $\ell_1$, the largest value of $\ell$ below which the LIF model cell always fires, approximately matches the observed threshold for $\ell$ in the HH model. Again, this is to make a reasonable comparison with the results from the HH model.

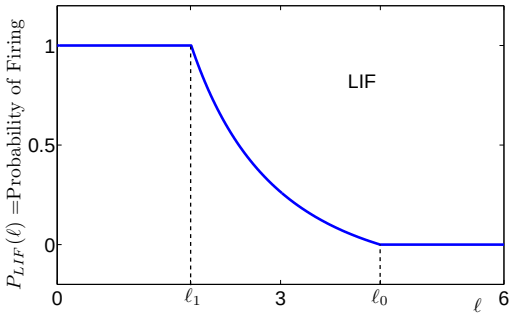


**Figure 4. Probability of firing as a function of $\ell$ for a Leaky-Integrate-and-Fire target neuron.** The first action potential arrives at the target neuron at $t = 0$ and the third action potential arrives at $t = \ell$. If $\ell \leq \ell_1$ the target neuron fires with probability one, and if $\ell > \ell_0$ the target neuron does not fire. $\ell_1$ and $\ell_0$ are quite far apart, so the LIF neuron does not have a sharp time window. For ease of comparison, we use a stimulus strength of $s = .4$ and the parameter $\tau$ for the LIF neuron was chosen so that $\ell_1$ matches the computed $\ell_1$ for the Hodgkin-Huxley neuron (Figure 3).

## 3. Leaky (Linear) Integrate-and-Fire Neurons.

We scale the voltage, $v$, of the LIF model so that $v = 0$ at rest and $v = 1$ is the threshhold at which the LIF neuron fires. We assume that each incoming action potential increases the voltage by $s$ and that $\frac{1}{3} \leq s < \frac{1}{2}$ since we want to study the $n = 3, m = 3$ case where three simultaneous hits would fire the LIF neuron but two simultaneous hits can not. We denote by $\tau$ the time constant of the LIF neuron, so $v(t)$ satisfies the differential equation $v'(t) = -\frac{1}{\tau}v(t)$.

We denote the arrival times of the the three incoming action potentials by $0, x, \ell$ respectively, so $\ell$ is the time between the first and third hits. Given $\ell$, we assume

that $x$ is uniformly distributed between 0 and $\ell$. We want to calculate $P_{LIF}(\ell)$, the probability that the target LIF neuron fires as a function of $\ell$. Since the stimuli are at $0, x$, and $\ell$, $v(t)$ is given by the the following formulas:

$$\begin{aligned} v(t) &= se^{-t/\tau}, \quad \text{for} \quad 0 \le t < x & (1)\\ v(t) &= (se^{-x/\tau} + s)e^{-(t-x)/\tau}, \quad \text{for} \quad x \le t < \ell & (2)\\ v(\ell) &= (se^{-x/\tau} + s)e^{-(\ell-x)/\tau} + s \quad \text{for} \quad t = \ell. & (3) \end{aligned}$$

We will denote the voltage at time $t = \ell$ by $H(x, \ell)$, so

$$H(x, \ell) \;=\; s(e^{-\ell/\tau} + e^{-(\ell-x)/\tau} + 1).$$

The LIF neuron will fire if and only if $H(x, \ell) \ge 1$.

Let $\ell_1$ denote that value of $\ell$ so that $P_{LIF}(\ell) = 1$ for all $\ell \le \ell_1$, i.e. the neuron fires with probability 1 independent of $x$. For fixed $\ell$, $H$ achieves its minimum at $x = 0$, so if $\ell \le \ell_1$, then $H(0, \ell) \ge 1$. Since $\ell_1$ is the largest $\ell$ that satisfies this inequality, $\ell_1$ satisfies $H(0, \ell_1) = 1$. Solving for $\ell_1$ yields:

$$\ell_1 \;=\; \tau \log\left(\frac{2s}{1-s}\right). \tag{4}$$

Let $\ell_0$ denote that value of $\ell$ so that $P_{LIF}(\ell) = 0$ for all $\ell \ge \ell_0$, i.e. the neuron fires with probability 0 independent of $x$. For fixed $\ell$, $H$ achieves its maximum at $x = \ell$, so if $\ell > \ell_0$, then $H(\ell, \ell) < 1$. Since $H(\ell, \ell)$ is strictly monotone decreasing in $\ell$, we see that $\ell_0$ satisfies $H(\ell_0, \ell_0) = 1$. Solving for $\ell_0$ yields:

$$\ell_0 \;=\; \tau \log\left(\frac{s}{1-2s}\right). \tag{5}$$

We note that $P_{LIF}(\ell_0) = 0$ even though $H(\ell_0, \ell_0) = 1$. because $x = \ell_0$ is the only value of $x$ so that $H(x, \ell_0) \ge 1$ and this event has probability zero.

In order to find $P_{LIF}(\ell)$ for $\ell_1 < \ell < \ell_0$, we have to find, for each $\ell^*$, the point $x^*$ so that $H(x^*, \ell^*) = 1$. This gives us the value for $x^*$ which is the boundary between values of x for which the cell will fire or fail to fire. The LIF neuron will fire if $x^* \le x \le \ell^*$, so $P_{LIF}(\ell^*) = \frac{\ell^* - x^*}{\ell^*}$ since we are assuming that the second hit is uniformly distributed between the first and the third. The point $(x^*, \ell^*)$ and the curve $H(x, \ell) = 1$ are shown in Figure 5A. Solving the equation $H(x^*, \ell^*) = 1$ yields:

$$x^* \;=\; \tau \log\left(\frac{1-s}{s} - e^{-\ell^*/\tau}\right) + \ell^*, \tag{6}$$

so,

$$P_{LIF}(\ell) = -\frac{\tau}{\ell}\log\left(\frac{1-s}{s} - e^{-\ell/\tau}\right). \tag{7}$$

The function $P_{LIF}(\ell)$ is graphed in Figure 4 for the case $s = .4$ and one can see clearly the gradual decline of $P_{LIF}(\ell)$ as $\ell$ goes from $\ell_1$ to $\ell_0$.

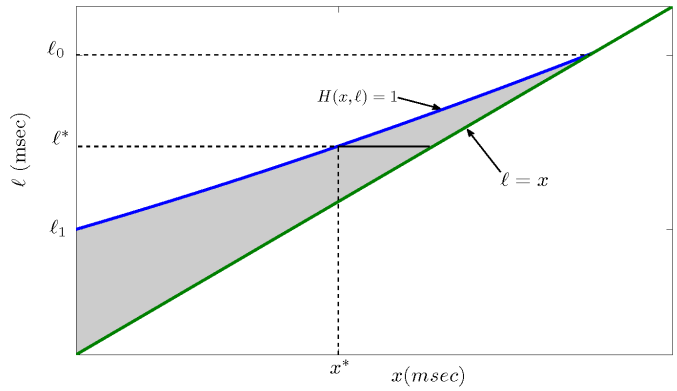


**Figure 5. Region of firing for the LIF neuron.** The vertical axis is $\ell$, the time between the arrival of the first and third action potentials. The horizontal axis is $x$, the arrival time of the second action potential. Suppose that $\ell = \ell^*$. The neuron will fire if $x^* \leq x \leq \ell^*$ (the thickened line) and will not fire if $x < x^*$. Since we are assuming that $x$ is uniformly distributed between 0 and $\ell^*$, the probability of firing is $\frac{\ell^* - x^*}{\ell^*}$. For $\ell < \ell_1$ the LIF neuron always fires and for $\ell > \ell_0$ the LIF neuron never fires. In between, it is more likely to fire if the second action potential is near the third. The stimulus strength is $s = .4$ and the value for $\tau$ is chosen so that $\ell_1 = 1.7$ (the value obtained for $\ell_1$ in HH)

In order to compare results for LIF and QIF neurons (Section 4), it is useful to compute the normalized spread defined as

$$W = \frac{l_0 - l_1}{l_1}.$$

The normalized spread gives the width of the interval $(\ell_1, \ell_0)$ relative to $\ell_1$. In this way it gives a dimensionless measure of the steepness of the drop from probability one to probability zero. Importantly, it also depends only on the parameter for stimulus strength, $s$, allowing a comparison of various models which is independent of the time constants. A short calculation shows that:

$$W_{LIF} = \frac{\log\left(\frac{(1-s)}{2(1-2s)}\right)}{\log\left(\frac{2s}{1-s}\right)}. \tag{8}$$

For $s = .4$, this gives a normalized spread of $W_{LIF} = 1.41$ for the LIF neuron. A comparison of $W_{LIF}$ with $W_{QIF}$ for all values of $s$ in the interval $[\frac{1}{3}, \frac{1}{2})$ is given in Figure 7.

## 4. Quadratic Integrate-and-Fire Neurons.

In this section we shall calculate $P_{QIF}(\ell)$, the probability of firing of a QIF neuron as a function of $\ell$, the time between the first and third arriving action potentials. As in Section 3, we scale the voltage, $v$, so that the neuron is at rest when $v = 0$ and and the threshold for firing is $v = 1$. All of the symbols introduced in Section 3, namely, $s, x, \ell, \ell_1, \ell_0$, and $H(x, \ell)$, have the same meanings here. The only difference is that the differential equation is now $v' = -\frac{1}{\tau}v(1 - v)$. Because this differential equation has an explicit solution we will be able to calculate, $\ell_1, \ell_0, P_{QIF}(\ell)$, and $W_{QIF}(s)$, but the calculations are somewhat more complicated. Since the stimuli are at times $0, x$, and $\ell$, the voltage is:

$$v(t) = \frac{se^{-t/\tau}}{1 - s + se^{-t/\tau}} \quad \text{for} \quad 0 \le t < x, \tag{9}$$

$$v(x) = \frac{se^{-x/\tau}}{1 - s + se^{-x/\tau}} + s, \tag{10}$$

$$v(t) = \frac{v(x)e^{-(t-x)/\tau}}{1 - v(x) + v(x)e^{-(t-x)/\tau}} \quad \text{for} \quad x \le t < \ell, \tag{11}$$

$$v(\ell) = \frac{v(x)e^{-(\ell-x)/\tau}}{1 - v(x) + v(x)e^{-(\ell-x)/\tau}} + s, \quad \text{for} \quad t = \ell. \tag{12}$$

Thus,

$$H(x, \ell) = \frac{\left(\frac{se^{-x/\tau}}{1-s+se^{-x/\tau}} + s\right) e^{-(\ell-x)/\tau}}{1 - \left(\frac{se^{-x/\tau}}{1-s+se^{-x/\tau}} + s\right) + \left(\frac{se^{-x/\tau}}{1-s+se^{-x/\tau}} + s\right) e^{-(\ell-x)/\tau}} + s$$

$H(x, \ell)$ gives the value of the voltage at $t = \ell$ if the second action potential arrives at $t = x$. Thus the QIF neuron fires if $H(x, \ell) \ge 1$. Suppose, for the moment that $x$ is fixed. If $v(x) + s < 1$ then the QIF neuron will not fire when the third action potential arrives. If $v(x) + s \ge 1$, then since $H(x, \ell)$ is strictly monotone decreasing to zero in $\ell$ there will be a unique largest $\ell$ so that $H(x, \ell) \ge 1$. We denote that $\ell$ by $\ell(x)$ and note that by continuity $H(x, \ell(x)) = 1$. Solving this equation yields:

$$\ell(x) = -\tau \log\left(\frac{1 - s}{s}\right) - \tau \log\left(\frac{1 - v(x)}{v(x)}\right) + x. \tag{13}$$

Recall that $\ell_1$ is that value of $\ell$ so that $P_{LIF}(\ell) = 1$ for all $\ell \leq \ell_1$, i.e. the QIF neuron fires with probability 1 independent of $x$. $\ell_1$ will be the smallest value of $\ell(x)$ as $x$ varies from 0 to $\bar{x}$, the value such that $v(\bar{x}) + s = 1$. To find the minimum we compute:

$$\ell'(x) \;=\; 1 + \frac{\tau}{v(x)(1-v(x))}\frac{d}{dx}v(x).$$

We note that $v(t)$ is not differentiable as a function of $t$ at $x$. However, the value of $v(t)$ at $x$, namely $v(x)$, is differentiable with respect to $x$ and that is the derivative that we mean above. Computing $\frac{d}{dx}v(x)$ and using (11) we find:

$$\ell'(x) \;=\; 1 - \frac{s(1-s)e^{-x/\tau}}{(s(1-s)+s(1+s)e^{-x/\tau})((1-s)^2 - s^2e^{-x/\tau})}.$$

Setting $\ell'(x) = 0$ and solving for $x$, a calculation shows that the critical point $x_1$ satisfies

$$e^{-x_1/\tau} \;=\; \frac{(1-s)^2}{s(1+s)},$$

so,

$$x_1 \;=\; \tau \log\left(\frac{s(1+s)}{(1-s)^2}\right).$$

Differentiating $\ell'(x)$ and collecting terms allows one to check that $\ell''(x_1) > 0$, so $x_1$ does indeed give the minimum. Plugging $x_1$ into $v(x)$ gives $v(x_1) = \frac{1+s}{2}$, and plugging both $x_1$ and $v(x_1)$ into (13) gives:

$$\ell_1 \;=\; \ell(x_1) \;=\; \tau \log\left(\frac{s^2(1+s)^2}{(1-s)^4}\right).$$

$\ell_0$ is the value of $\ell$ above which $P_{QIF}(\ell) = 0$; thus $\ell_0$ is the maximum of $\ell(x)$ on the interval $[0, \bar{x}]$. A calculation shows that $\ell(x)$ is concave upwards so the maximum occurs at one of the endpoints. First we solve $v(\bar{x}) + s = 1$ to find $\bar{x}$. Evaluating $\ell(0)$ and $\ell(\bar{x})$, we find that the values are both the same and equal to:

$$\ell_0 \;=\; \tau \log\left(\frac{2s^2}{(1-s)(1-2s)}\right).$$

Figure 6A shows the graph of the function $\ell(x)$, the points $x_1$ and $\bar{x}$, and the heights $\ell_1$ and $\ell_0$. The shaded region are the pairs $(x, \ell)$ such that the QIF neuron fires.

We have computed $\ell_1$ and $\ell_0$ and we know that $P_{QIF}(\ell) = 1$ if $\ell \leq \ell_1$ and $P_{QIF}(\ell) = 0$ if $\ell \geq \ell_0$. For $\ell_1 < \ell < \ell_0$ we expect two points, $x_-$,$x_+$, so that $\ell(x_-) = \ell$ and $\ell(x_+) = \ell$ (see Figure 6A). The value of $P_{QIF}(\ell)$ is then given by

$$P_{QIF}(\ell) \;=\; \frac{x_- + (\ell - x_+)}{\ell}, \tag{14}$$

the fraction of the line from $(0, \ell)$ to $(\ell, \ell)$ that lies in the shaded region since we are assuming that the time of the second action is uniformly distributed between 0 and $\ell$. To find $x_-$ and $x_+$, we rewrite (13) as

$$e^{-(\ell - x)/\tau} \;=\; \left(\frac{1-s}{s}\right)\left(\frac{1-v(x)}{v(x)}\right).$$

Substituting for $v(x)$ and rearranging gives

$$e^{-(\ell - x)/\tau} \;=\; \left(\frac{1-s}{s}\right)\left(\frac{(1-s)^2 - s^2 e^{-x/\tau}}{s(1-s) + s(1+s)e^{-x/\tau}}\right).$$

Multiplying out yields a quadratic in $e^{-x/\tau}$ whose solutions,

$$e^{-x_\pm/\tau} \;=\; \frac{1}{2}\left\{\left(\frac{1-s}{s}\right)^2 - e^{-\ell/\tau}\left(\frac{1+s}{1-s}\right) \mp \sqrt{\left(\left(\frac{1-s}{s}\right)^2 - e^{-\ell/\tau}\left(\frac{1+s}{1-s}\right)\right)^2 - 4e^{-\ell/\tau}}\right\},$$

give the $x_-$ and $x_+$ used in (14). The graph of $P_{QIF}(\ell)$ is shown in Figure 6B.

Finally, the normalized spead , $W_{QIF} = \frac{\ell_0 - \ell_1}{\ell_1}$, for the QIF neuron is given by:

$$W_{QIF} \;=\; \frac{\log\left(\frac{2(1-s)^3}{(1-2s)(1+s)^2}\right)}{\log\left(\frac{s^2(1+s)^2}{(1-s)^4}\right)}.$$

As in the case of the LIF neuron, the normalized spread does not depend on $\tau$. For $s = .4$ the formula gives a normalized spread of $W = .18$, so the QIF neuron has a very sharp time window as is also clear by Figure 6B. The case $s = .4$ is not special. Figure 7 shows $W_{LIF}$ and $W_{QIF}$ for all $s$ in the interval $[\frac{1}{3}, \frac{1}{2})$.

## 5. Discussion.

In Sections 3 and 4, our explicit calculations show that the LIF neuron does not have a sharp time window but the QIF does have a very sharp time window. Here is some intuition that helps explains why this is true. Set $\tau = 1$ and $s = 0.4$ and

consider the LIF neuron first. If the first two action potentials arrive at the same time, then $v$ jumps to .8 at $t = 0$. The third action potential must arrive before $v$ decays to 0.6, and that will be a relatively short time since $v' = -v$, $v(0) = 0.8$, and $v$ will decay rapidly. However, if the second and third action potentials arrive together, then $v' = -v$ and $v(0) = 0.4$, and they must arrive before $v$ decays to 0.2. This decay will take much longer than in the previous case because $v$ is so much smaller. Thus, for LIF we expect $\ell_1$ and $\ell_0$ to be quite far apart, which is what we see in the formulas (4) and (5), and in the normalized spread, $W_{LIF}$, in Figure 7. On the other hand, for the QIF neuron the right hand side of the differential equation, $-v(1-v)$ curves back up to 0 as $v$ approaches 1 and its value is not so different at 0.4 and at 0.8. Thus, the decay rates will be quite similar and we expect that $\ell_1$ and $\ell_0$ will be close together. This gives some understanding of why the Hodgkin-Huxley model and other non-linear models that we have experimented with have fairly sharp time windows. The strength of the decay back to the stable equilibrium after one action potential arrives is not so different from the strength of the decay after two have arrived because the vector field becomes smaller as one approaches the higher unstable equilibrium. We also note that the time of firing will vary accross models. In LIF and QIF, the target cell fires exactly at the time of the third input. In HH and other biophysically detailed models, firing is not instantaneous. However, preliminary numerical results indicate that time of firing changes only slightly except in the border cases where the final input pushes the target cell only slightly past the unstable manifold.

We have compared different models in the case $n = 3$, $m = 3$, that is, there are three afferent fibers and three hits are required to fire the target neuron. As discussed at the beginning of Section 2, this is the simplest case where one would expect that different models would have different behavior. When $n = m > 3$, explicit calculations become more difficult but we can continue to plot probability of firing as a function of $\ell = t_n - t_1$ and compute $\ell_1$, $\ell_0$ and $W$. Figure 8 shows numerical calculations for the case $n = m = 4$ when we assume that the second and third hits are uniformly distributed between the first and the fourth. The probability curves for the QIF model and the Hodgkin-Huxley model drop rapidly, not as rapidly as in the case $n = m = 3$, but still much more rapidly than the probability curve for the LIF model. In the case $m < n$ a higher dimensional comparison is required. One must determine which points $(t_2 - t_1, t_3 - t_1, \ldots, t_n - t_1)$ in $\mathbb{R}^{n-1}$, lead to successful firings (as we did in Figures 5 and 6). Analytical results and further numerical simulations for the cases $n = m > 4$ or $m < n$ are required to determine whether the time window behaviors we have found for various models extend to these cases also.

We note that TW neurons and LIF neurons are the same in certain asymptotic limits. An LIF neuron also has two parameters, the strength of the input $\frac{V_i}{V_{thr}}$, where $V_i$ is the change in post-synaptic membrane voltage caused by each incoming action potential and $V_{thr}$ is the voltage required to fire the target cell, and the time constant, $\tau$. In the asymptotic limit where $\tau \to \infty$, the LIF neuron fires when it has received $\geq \frac{V}{V_i}$ inputs (an IF neuron). Similarly, in the asymptotic limit where $\varepsilon \to \infty$, the

TW neuron will fire when the $m$th hit arrives. Thus in these two special asymptotic limits the two models are the same and the distribution of the time of firing of the target cell is given by the $m$th order statistic (which will depend on the convergence, $n$, and input density $f$).

For several reasons, simple models of individual neurons are useful for studying complex behavior in the central nervous system. Simple models use less computational power. If one uses more complex full biophysical models, it may be difficult to discern whether observed behavior results from network properties or individual neuron properties. And, finally, if the models for individual neurons are sufficiently simple, one may actually be able to prove theorems about the origin of the system behavior under study. Of course, simple models like TW or LIF cannot capture the complex behavior of full biophysical models. And, physiological behavior probably depends on network properties, on channel properties, on anatomy through the detailed arrangement of synapses on the target cell, and on learning. Indeed, Azouz and Gray [2] and Bal and Oertel [3] have shown how specific channel properties enhance coincidence detection and Golding et al [21] showed how the serial arrangement of AN fibers on the dendrites of octopus cells compensates for the wave delay on the cochlea allowing for excellent coincidence detection. Gerstner et al [18] proposed that coincidence detection could be learned through Hebbian rules and Grothe [14] has provided evidence of developmental changes to improve coincidence detection in the medial superior olive of gerbils. Nevertheless, it is useful and important to use simple neural models, like LIF or TW, to investigate how network properties contribute to coincidence detection and the synchronous firing of subpopulations of neurons. The analytical and numerical results of this paper show that the Hodgkin-Huxley model and the QIF model have sharp time windows similar to the TW neuron (at least in the case $n = m = 3$), while the LIF neuron does not have a sharp time window. This suggests that if one is studying how synchrony or coincidence detection arises from network structure in the presence of noise or neuronal jitter, it may be more appropriate to use TW neurons than LIF neurons.

In addition to the work on the auditory nerve and cochlear nucleus cited in the Introduction, there have been many other interesting and insightful investigations of the network properties that give rise to synchrony and coincidence detection. In the theory of synfire chains, proposed by Abeles [1] and developed by many others (for example [13][39][22]) for studying cortical circuits, the networks have both noise and high convergence from level to level. Brunel and coworkers have studied, both analytically and computationally, the emergence of synchrony in sparsely connected networks [6][5], and also how synaptic noise affects the frequency response of spiking neurons [7]. Kempter, Gerstner, and van Hemmen investigated how the capacity for coincidence detection depends on the membrane time constant and the threshold [27] and how the synchrony of the output depends on neural parameters and jitter parameters [28]. Kopell and Ermentrout investigated the complementary roles of excitatory and inhibitory synapses in networks that have the capacity for synchronous oscilla-

tions [30] and Borgers and Kopell investigate conditions under which sparse random connectivity can give rise to synchronous oscillations [4]. Marinazzo et al [31] have suggested that if synapses are allowed to be dynamic then excitatory-inhibitory networks can encode both temporal characteristics of the input and spatial correlations. Except for [30] and [4], which used QIF neurons and the the theta-model, most of these modeling studies used LIF neurons. It would be very interesting to redo some of these investigations with TW neurons instead of LIF neurons, because the results presented here suggest that synchrony and coincidence detection will be improved with TW neurons and that some physiological neurons may behave approximately like TW neurons.

Finally, we note that Rochel and Cohen [42] have raised the very interesting question of whether networks themselves could have time windows. This is particularly important if the network receives a continuous stream of time varying inputs that the network turns into population codes that must be read out in real time by a higher level system. The population representation of the temporal pattern should last only a short time so that it can be replaced by the next pattern. It would be interesting to investigate how such network time windows could be created by inhibition.

This paper is about models. It would be very interesting if experimentalists could determine how sharp the time windows of different types of physiological neurons are. There is some evidence for sharp time windows. If the Hodgkin-Huxley equations represent the physiology of the squid giant axon well, then the squid giant axon has a sharp time window, at least in the case $n = 3, m = 3$. Ferragamo and Oertel [16] have conducted a detailed study of the potential of the post-synaptic membrane of octopus cells in the CN that require many incoming action potentials from different AN fibers to fire. They showed that it is the rate of rise of the potential (dependent on the rate of arrival of incoming spikes) that determines whether the octopus cell fires. This is exactly what one would expect if the octopus cell had a sharp time window. If the rate of rise is high enough then there will be enough incoming spikes in the time window and if the rate of rise is too slow then there will not be enough incoming spikes in the time window.

## Acknowledgments.

The research in the paper and its preparation were supported by NSF grants #DMS-0109872 and #DMS-0616710.

# References

[1] M. ABELES (1991), Corticonics: Neural Circuits of the Cerebral Cortex, Cambridge University Press, Cambridge, UK.

[2] R. AZOUZ and C. Gray (2000), Dynamic spike threshold reveals a mechanism for synaptic coincidence detection in cortical neurons *in vivo*, PNAS, 97, 8110-8115.

[3] R. BAL and D. OERTEL, (2000), Hyperpolarization-activated, mixed-cation current ($I_h$) in octopus cells of the mammalian cochlear nucleus, J. Neurophysiol. 84, 806-817.

[4] C. BORGERS and N. KOPELL, 2003, Synchronization in networks of excitatory and inhibitory neurons with sparse, random connectivity, Neural Computation, 15, 509-538.

[5] N. BRUNEL, 2000, Dynamics of sparsely connected networks of excitatory and inhibitory spiking neurons, J. Computational Neuroscience, 8, 183-208.

[6] N. BRUNEL and V Hakim, 1999, Fast global oscillations in networks of integrate-and-fire neurons with low firing rates, Neural Computation, 11, 1621-1671.

[7] N. Brunel, F. Chance, N. Fourcaud, and L. F. Abbott, 2001, Effects of synaptic noise and filtering on the frequency response of spiking neurons, Physical Review Letters, 86, 2186-2189.

[8] A. BURKITT and G. CLARK, (1999), Analysis of Integrate-and-fire neurons: synchronization of synaptic input and spike output, Neural Computation 11, 871-901.

[9] A. BURKITT and G. CLARK, (2001), Synchronization of the neural response to noisy periodic synaptic input, Neural Computation 13, 2639-2672.

[10] Y. CAI, E. WALSH, and J. MCGEE, (1997), Mechanisms of Onset Responses in Octopus Cells of the Cochlear Nucleus: Implications of a Model, J. Neurophysiol. 78, 872-883.

[11] Y. CAI, J. MCGEE, and E. WALSH, (2000), Contributions of Ion Conductances to the Onset Responses of Octopus Cells in the Ventral Cochlear Nucleus: Simulation Results, J. Neurophysiol. 83, 301-314.

[12] E. COVEY and J. H. CASSEDAY, (1991), The monaural nuclei of the lateral lemniscus of the echolocating bat: Parallel pathways for analyzing the temporal features of sounds, J. Neurosci. 11, 3456-3470.

[13] M. DIESMANN, M-O GEWALTIG, S. ROTTER, and A. AERSTED, (1999), Stable propagation of synchronous spiking in cortical neural networks, Nature 402, 529-533.

[14] B. GROTHE, 2003, New roles for synaptic inhibition in sound localization, Nature Reviews Neuroscience, 4, 4-11.

[15] G. B. ERMENTROUT and N. KOPELL, (1986), Parabolic Bursting in an Excitable System Coupled with a Slow Oscillation, SIAM J. Appl. Math. 46, 233-253.

[16] M. FERRAGAMO and D. OERTEL, (2003), Octopus cells of the Mammalian Cochlear Nucleus Sense the Dynamic Properties of Synaptic Excitation, J. Neurophysiol. 87, 2262-2270.

[17] R. FITZHUGH, (1955), Mathematical models of threshold phenomena in the nerve membrane, Bull. Math. Biophysics 17, 257–278

[18] W. GERSTNER, R. KEMPTER, J. van HEMMEN, and H. Wagner, (1996), A neuronal learning rule for sub-millesecond temporal coding, Nature, 383, 76-78.

[19] J. M. GOLDBERG and P. B. BROWN, (1969), Response of binaural neurons of dog superior olivary complex to dichotic tone stimuli: some physiological mechanisms of sound localization, J. Neurophysiol. 32, 613-636.

[20] N. GOLDING, D. ROBERTSON, and D. OERTEL, (1995), Recordings from slices indicate that octopus cells of the cochlear nucleus detect coincident firing of auditory nerve fibers with temporal precision, J. Neurosci. 15, 3138-3153.

[21] N. GOLDING, M. Ferragamo, and D. OERTEL, (1999), Role of intrinsic conductances underlying responses to transients in octopus cells of the cochlear nucleus, J. Neurosci. 19, 2897-2905.

[22] G. HAYON, M. ABELES, and D. LEHMANN, (2005), A model for representing the dynamics of a system of synfire chains, J. Comp. Neurosci. 18, 41-53.

[23] A. L. HODGKIN and A. F. HUXLEY, (1952), A quantitatinve description of membrane current and its application to conduction and excitation in nerve, J. Physiol. 117, 500-544.

[24] L. A. JEFFRESS, (1947), A place theory of sound localization, J. Comp. Psychol. 41, 35-39.

[25] S. KALLURI and B. DELGUTTE, (2003), Mathematical models of cochlear onset neurons: I. point neuron with many synaptic inputs, J. Comp. Neurosci. 14, 71-90.

[26] S. KALLURI and B. DELGUTTE, (2003), Mathematical models of cochlear onset neurons: II. model with dynamic spike-blocking state, J. Comp. Neurosci. 14, 91-110.

[27] R. KEMPTER, W. GERSTNER, and J. L. van HEMMEN, 1998, How the threshold of a neuron determines its capacity for coincidence detection, BioSystems, 48, 105-112.

[28] R. KEMPTER, W. GERSTNER, J. L. van HEMMEN, and H. Wagner, 1998, Extracting oscillations: neuronal coincidence detection with noisy periodic spike input, Neural Computation, 10, 1987-2017.

[29] N. KIANG, (1996), Discharge Patterns of Single Fibers in the Cat's Auditory Nerve, MIT press, Cambridge.

[30] N. KOPELL and B. Ermentrout, (2004), Chemical and electrical synapses perform complementary roles in the synchronization or interneuronal networks, PNAS 101, 15482-15487.

[31] D. MARINAZZO, H. J. KAPPEN, S. C. A. M. GIELEN, 2007, Input-driven oscillations in networks with excitatory and inhibitory neurons with dynamic synapses, Neural Computation, 19, 1739-1765.

[32] C. MITCHELL, (2003) Mathematical Properties of Time-windowing in Neural Systems, Duke University Thesis.

[33] C. MITCHELL, (2005) Precision of neural timing: the small $\varepsilon$ limit, J. Math. Anal, Appl. 309, 567-582.

[34] C. MITCHELL and M. REED, (2007) Neural timing in highly convergent systems, SIAM J. Appl. Math. 68,720-737.

[35] D. OERTEL, R. BAL, S. GARDNER, P. SMITH, and P. JORIS, (2000), Detection of synchrony in the activity of auditory nerve fibers by octopus cells of the mammalian cochlear nucleus, PNAS 97, 11773-11779.

[36] G. D. POLLAK, (1993), Some comments on the perception of phase and nanosecond time disparities by echolocating bats, J. Comp. Physiol. A. 172, 523-531.

[37] L. RAYLEIGH, (J. W. Strutt), (1907) On our perception of sound direction, Phil. Mag. 13, 214-232.

[38] M. REED, J. BLUM, and C. MITCHELL, (2002), Precision of neural timing: effects of convergence and time-windowing, J. Comp. Neurosci. 13, 35-47.

[39] A. REYES, (2003), Synchrony-dependent propagation of firing rate in iteratively constructed networks *in vitro*, Nature Neurosci. 6, 593-599.

[40] W. S. RHODE, D. OERTEL, and P. H. SMITH, (1983), Physiological response properties of cells labelled intracellularly with horseradish peroxidase in cat ventral cochlear nucleus, J. Comp. Neurol. 213, 448-463.

[41] W. S. RHODE and P. H. SMITH, (1986), Encoding timing and intensity in the ventral cochlear nucleus of the cat, J. Neurophysiol. 56, 261-286.

[42] O. ROCHEL and M. COHEN, (2007), Real time computation: Zooming in on population codes, BioSystems 87, 260-266.

[43] J. S. ROTHMAN and P. B. MANIS, (2003), Differential expression of three distinct potassium currents in the ventral cochlear nucleus, J. Neurophysiol. 89, 3070-3082

[44] J. S. ROTHMAN and P. B. MANIS, (2003), Kinetic analyses of three distinct potassium conductances in ventral cochlear nucleus neurons, J. Neurophysiol. 89, 3083-3096

[45] J. S. ROTHMAN amd P. B. MANIS, (2003), The roles potassium currents play in regulating the electrical activity of ventral cochlear nucleus neurons, J. Neurophysiol. 89, 3097-3113

[46] J. ROTHMAN, E. YOUNG, and P. MANIS, (1993), Convergence of auditory nerve fibers onto bushy cells in the ventral cochlear nucleus: implications of a computational model, J. Neurophysiol. 70, 2562-2582.

[47] J. ROTHMAN, and E. YOUNG, (1996), Enhancement of neural synchronization in computational models of ventral cochlear nucleus bushy cells,. J. Auditory Neuroscience 2, 47-62.

[48] J. A. SIMMONS, M. FERRAGAMO, C. F. MOSS, S. B. STEVENSON, and R. A. ALTES, (1990), Discrimination of jittered sonar echoes by the echolocating bat, *Eptesicus fuscus*: The shape of target images in echolocation, J. Comp. Physiol. A. 167, 589-616.

[49] W. YOST and G. GOUREVITCH, eds., (1987), Directional Hearing, Springer-Verlag, New York.

[50] E. YOUNG, J.-M. ROBERT, and W. SCHOFNER, (1988), Regularity and latency of units in ventral cochlear nucleus: implications for unit classification and generation of response properties, J. Neurophysiol. 60, 1-29.

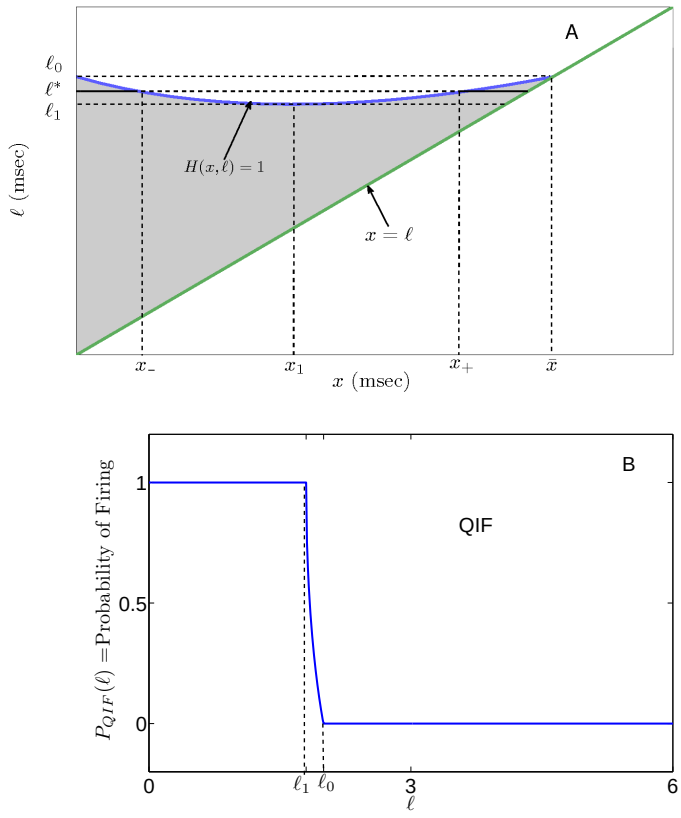


**Figure 6. The QIF neuron.** Panel A shows the region of firing for the QIF neuron. The vertical axis is $\ell$, the time between the arrival of the first and third action potentials. The horizontal axis is $x$, the arrival time of the second action potential. Suppose that $\ell = \ell^*$. The QIF neuron will fire if either $0 \leq x \leq x_-$ or $x_+ \leq x \leq \ell^*$ (thickened lines). Since $x$ is assumed to be uniformly distributed between 0 and $\ell^*$, the probability of firing is $\frac{x_- + (\ell^* - x_+)}{\ell^*}$. For $\ell < \ell_1$ the QIF neuron always fires and for $\ell > \ell_0$ the QIF neuron never fires. In between, it is more likely to fire if the second action potential is near either the first or the third. Panel B shows the probability of firing of the QIF neuron as a function of $\ell$. Since $\ell_1$ and $\ell_0$ are quite close, the QIF neuron behaves similarly to the time window neuron and the Hodgkin-Huxley neuron. The stimulus strength is again $s = .4$ and the value for $\tau$ is chosen so that $\ell_1 = 1.7$ (the value obtained for $\ell_1$ in HH)

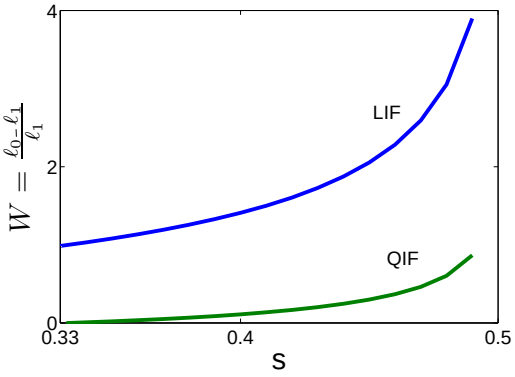


**Figure 7. Normalized spread.** The two curves show the normalized spread $W(s) = \frac{\ell_0 - \ell_1}{\ell_1}$ as a function of $s$ for the LIF and QIF neurons. The stimulus strength $s$ is required to be between $\frac{1}{3}$ and $\frac{1}{2}$ of threshold in the case $n = 3, m = 3$.

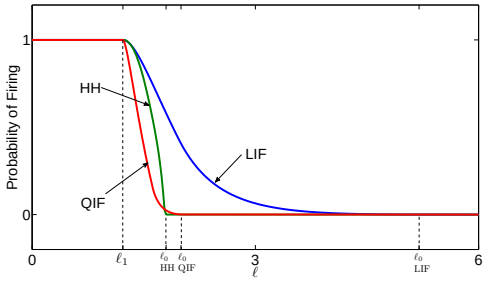


**Figure 8. The case $n = m = 4$.** Probability of firing as a functions of $\ell$ where $\ell$ is the time between the first and fourth hits. The stimulus strength $s = 0.3$ was chosen to be between $\frac{1}{4}$ and $\frac{1}{3}$. The values for the time constants for LIF and QIF were chosen so that all three models have the same value for $\ell_1$. The value of $\ell_1 = 1.2$, and the values for $\ell_0$ for all three models are shown (approximately 1.8 for HH, 2.0 for QIF and 5.2 for LIF) are shown. Again, HH and QIF have much sharper time windows than LIF.